RSC Advances

PAPER

Cite this: *RSC Adv.*, 2023, **13**, 31659

Robust reverse-electrowetting based energy harvesting on slippery surface†

Haimei Cheng,[ab] Wan Shao,[ab] Jing Jin,[ab] Junjun Wu,[ab] Manhong Zhao,[ab] Biao Tang *[ab] and Guofu Zhou[abc]

Received 7th September 2023
Accepted 25th October 2023

DOI: 10.1039/d3ra06099c

rsc.li/rsc-advances

Reversed-electrowetting based droplet electricity generator (REWOD-DEG) shows merits in high power densities, tunable output formats, and wide adaptability to diverse mechanical energies. However, the surface charge trapping and dielectric failure, which are also common challenges for electrowetting system, hinders the development of reliable REWOD-DEGs for long-term running. We innovatively introduce a slippery lubricant-infused porous surface (SLIPS) into REWOD-DEG. Benefits from the significant inhibitory effect for surface charge trapping and ambient contamination, self-healing characteristic given by SLIPS, and robust reversed-electrowetting based energy harvesting were achieved. The SLIPS enhanced REWOD-DEG experienced 100 days of intermittent energy harvesting without deterioration. In addition, the device shows robust performances when exposed to a variety of extreme working conditions, like low temperature, pH, humidity, fouling, and even scratching. This work may address the core application challenges of REWOD based devices, and inspire the development of other robust droplet-based electricity generators.

1 Introduction

Water in nature contains tremendous kinetic energy, which is clean, renewable, and collectible; the advancement of green energy and micro/nano manufacturing technology has led to a growing interest in researching the harvesting of mechanical energy in liquid environments.[1–4] The conversions include triboelectric nanogenerators (TENG),[5–8] electrokinetic effect generator (EKEG),[9,10] piezoelectric nanogenerator (PENG),[11,12] electrical double layer capacitor (EDLC),[13,14] and reversed electrowetting (REWOD) based electricity generator,[15,16] *etc.* Among them, reversed-electrowetting based droplet electricity generator (REWOD-DEG) shows great advantages in high power densities (up to 10^3 W m^{-2}), tunable output formats (several volts to tens of volts), and wide adaptability to diverse mechanical energies, such as energy harvesting from human movement and high-power generation from mechanical vibration, which supports promising application in portable, wearable devices.[17–19]

As a solid/liquid capacitive power generation device with bias voltage, the performance of REWOD-DEG is limited by wetting behavior and the inherent charge trapping and dielectric failures of the electrowetting system.[18–20] Up to date, oil infused slippery surface has been introduced in variety EWOD or droplets energy harvesting applications,[21–24] its unique advantages given by the fluidic nature, such as low contact angle hysteresis, antifouling, self-healing and liquid repellency have been extensively studied. However, the dielectric properties of SLIPS film as a liquid dielectric layer was rarely reported. In our previous studies, we found the ion barrier effect of SLIPS in an electrowetting system,[25] which lights up the potential to address the crucial issue of charge trapping in reverse electrowetting (REWOD) based devices.

This work innovatively introduced SLIPS into REWOD based droplet electricity generator for robust mechanical energy harvesting. The stability in long-time running and the tolerance to extreme operating conditions for the SLIPS enhanced REWOD-DEG were systematically studied.

2 Results and discussion

2.1 Characterizations of SLIPS

The slippery surface was prepared by spin-coating a lubricant onto a polytetrafluoroethylene (PTFE) film covered on an indium tin (ITO) glass (see Fig. 1a). The lubricant with low surface tension easily infuses into the porous PTFE (Fig. 1b) and forms SLIPS, which is immiscible with most liquids.[26] The SLIPS film shows much higher transmittance compared to the

[a]*Guangdong Provincial Key Laboratory of Optical Information Materials and Technology & Institute of Electronic Paper Displays, South China Academy of Advanced Optoelectronics, South China Normal University, Guangzhou 510006, People's Republic of China. E-mail: tangbiao@scnu.edu.cn*

[b]*National Center for International Research on Green Optoelectronics, South China Normal University, Guangzhou 510006, People's Republic of China*

[c]*Shenzhen Guohua Optoelectronics Tech. Co. Ltd, Shenzhen 518110, People's Republic of China*

† Electronic supplementary information (ESI) available. See DOI: https://doi.org/10.1039/d3ra06099c

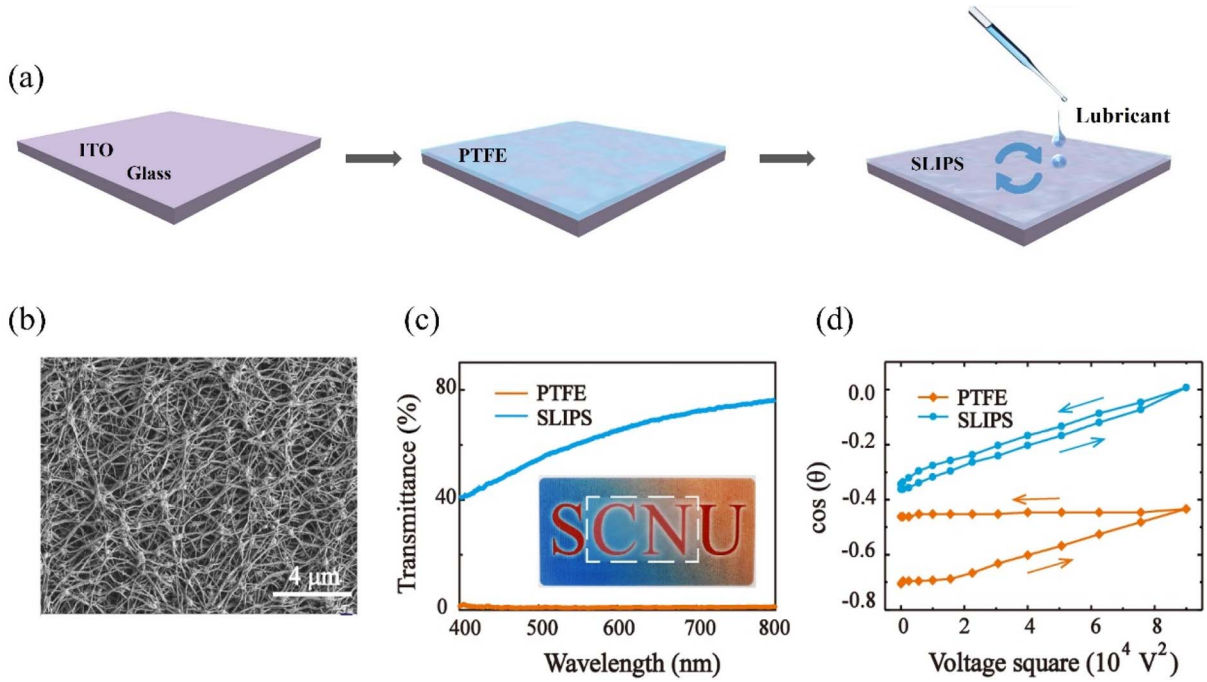

Fig. 1 Characterization of the slippery surface (SLIPS). (a) Schematic drawing of SLIPS fabrication process, (b) SEM image of the PTFE membrane, (c) transmittance measurements of SLIPS film and original PTFE film, insert shows a SLIPS covered glass (inside the white dashed rectangular box) siting on a paper with printed characters, (d) the electrowetting behavior on pre-charged PTFE and SLIPS.

original PTFE film (Fig. 1c). As shown in the insert, the text below can be clearly seen through the SLIPS covered glass. The lubricant liquid fills the air pockets in the porous film, reducing light scattering at the surface/air interface,[27] which can explain the enhancement in transmittance.

A harsh charge trapping test of SLIPS and PTFE was conducted using the electrowetting-assistant surface charging method.[28,29] The surface of samples was charged under a 400 V bias applied between sample electrode and the aqueous solution (ESI: Fig. S1†). As widely agreed, the trapped charges on the surface will directly cause the electrowetting curve deviation from the theoretical prediction by the Young–Lipmann equation.[30–34] The data in Fig. 1d shows a linear and reversible electrowetting behavior on SLIPS, while a significant decline in droplet manipulation performance occurs on PTFE. The obvious symmetry differences of electrowetting curves (Fig. S2†) also indicates the introduction of SLIPS blocks surface charge trapping, which can be explained by the extra insulation effect given by the perfect oil-infusion to the pores inside PTFE.

2.2 SLIPS based REWOD-DEG performance

The REWOD-DEG comprises a conducting liquid and a parallel conducting electrode substrate covered with a dielectric layer. A droplet is placed between two electrodes, and the distance between them is altered through mechanical modulation in the form of sinusoidal vibrations, achieved by vertically vibrating the bottom plate (Fig. 2a). The electrodes are linked to an external power source and the output of the system is tested by measuring the voltage drop across the load resistor R_L. It should be noted that the wetting characteristics of the two conductive plates differ entirely. Specifically, the upper plate is covered with SLIPS, while the lower plate consists of a purely conductive ITO. Therefore, in this experiment, the upper plate is hydrophobic and the lower plate is hydrophilic. The circuit of the system is represented by an equivalent variable capacitor and a resistor connected in series, while an applied bias power supply is present (Fig. 2b). In terms of charge transfer, the process works as follows: initially, the lower electrode plate is positively charged due to the positive power supply. At the interface, the droplet and the lower electrode plate are electrostatically induced and negatively charged, forming a double-layer capacitance. The lower electrode plate and the droplet also form another double-layer capacitance to maintain system balance. As the lower plate vibrates, it increases the contact area with the droplet, attracting more positive charge from the power source. This movement of charge creates a current. Conversely, as the contact area decreases, the charge flows back and a reverse current is formed (Fig. 2c and d).

In REWOD-DEG, the electrical energy generated per unit area at the interface of the liquid-thin film dielectric-solid is directly proportional to the interface capacitance.[16] Therefore, the AC current generation in REWOD-DEG dependents on various parameters, including droplet concentration, vibration frequency and amplitude, applied voltage, and load resistance. The capacitance in the dielectric material is directly or indirectly affected by these parameters, which in turn affects the output of the energy collector. The REWOD-DEG process can be optimized by choosing the right conductive liquid and polymer coating to reduce the effects of contact angle hysteresis and

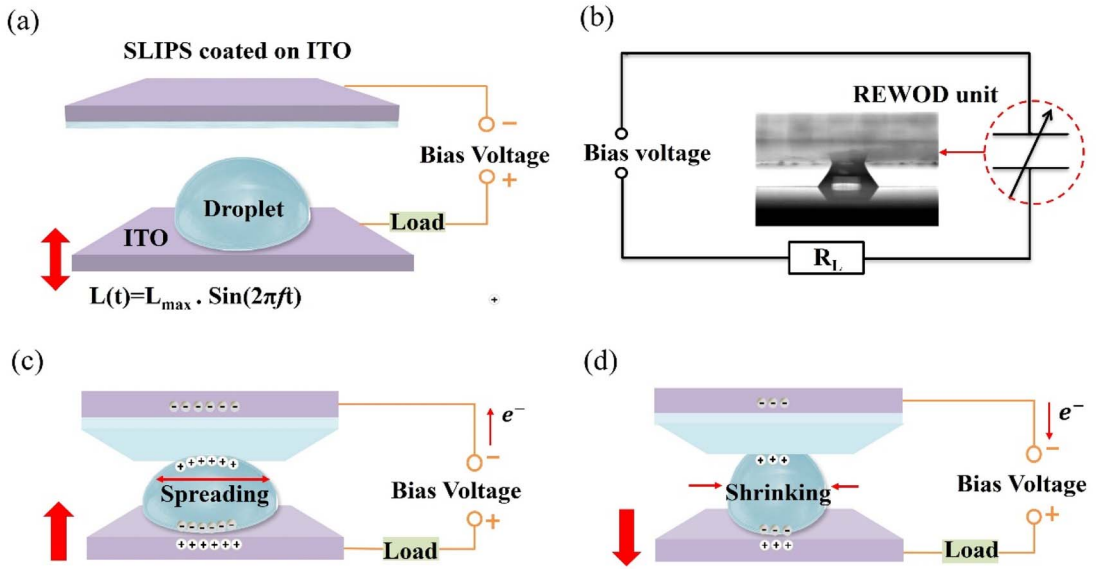

Fig. 2 Schematic diagram of the experiment and circuit model. (a) Experimental setup, (b) circuit model of REWOD-DEG (inset: video image of water bridge), (c) when the droplet start to contact the plate and (d) at the very moment when the two plates are approaching each other.

charge trapping.[35–37] Common ionic liquids such as ultrapure water and NaCl solution (0.5 mol L^{-1}, 1 mol L^{-1}) were used in this experiment.

As expected, higher concentrations resulted in slight increase in V_{rms} (the root mean square value of the voltage distributed on the load resistance V_L) compared to pure water (Fig. 3a). This can be attributed to the increase in mobile ion density, resulting in higher capacitance. Based on the essence of a variable capacitor for REWOD-DEG, high concentration solutions with high conductivity are preferred for pursuing high

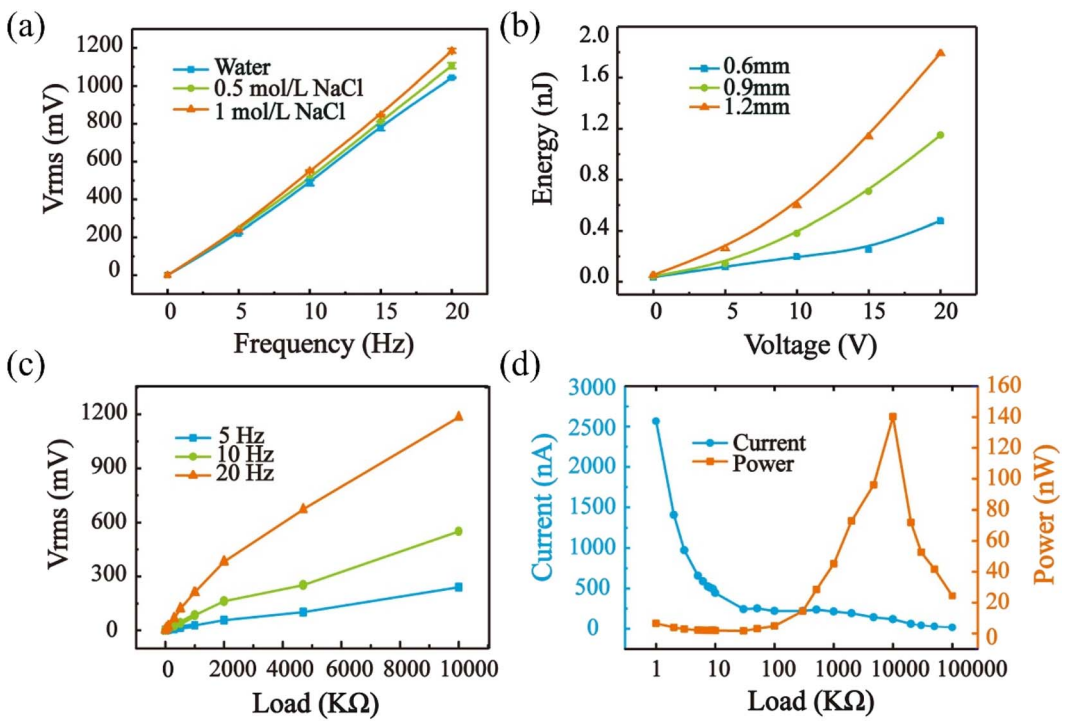

Fig. 3 The energy output performance of REWOD-DEG under various working conditions. (a) The effects of vibration frequency and solution differentiation on the output V_{rms}, $R_L = 10$ MΩ, $L = 1.2$ mm, $V = 20$ V. (b) Energy generated per vibration cycle as a function of bias voltage at different vibration amplitude, $R_L = 10$ MΩ, $f = 5$ Hz. (c) Load resistance and vibration frequency effect on V_{rms}, $V = 20$ V, $L = 1.2$ mm. (d) Load resistance effect on power and current outputs. $f = 20$ Hz, $V = 20$ V, $L = 1.2$ mm. For all graphs, the droplet volume is 10 μL.

power output.[16,17] Therefore, in all subsequent experiments, unless otherwise specified, the high concentration NaCl solution of 1 mol L^{-1} was applied as the liquid choice. We studied the influence of driving waveform applied to vibrator on the energy output of REWOD-DEG. By comparing square wave, sine wave, and triangular wave, we found that sine waves give more stable and higher energy outputs, especially at a frequency of 5 Hz perform best (Fig. S3†). It is obvious that regardless of the type of droplets, the output voltage increases with the frequency increases (Fig. 3a). Limited by the hydrodynamic response,[38] the vibration frequencies used in our experiments did not exceed 20 Hz which are common movement frequency in daily life.

The energy generated per vibration cycle as a function of bias voltage at different vibration amplitude is presented in Fig. 3b. As we discussed, to a REWOD-DEG, the appliable output energy is highly correlated to the energy changes in the equivalent capacitor, which can be written as $\frac{1}{2}\Delta CV^2$. Therefore, a higher bias voltage or a larger change in solid/liquid contacts lead to higher amount of energy generated per vibration cycle. The trend of V_{rms} outputs changing with load resistance was presented in Fig. 3c, in which the V_{rms} outputs shows monotonic increase with vibration frequency and load resistance. By carefully choosing the working conditions, particularly the load condition, we got the maximum peak power of 143 nW (Fig. 3d). The REWOD-DEG shows potential application by lighting up LED lights based on droplet array approach (Fig. S4†).

2.3 Robust energy harvesting

The accumulative trapped charges in the dielectric layer will decline the stability of the current generation of the REWOD-DEG system.[39] As shown in Fig. 4a, the SLIPS based REWOD-DEG shows very stable electricity output V_L withstanding 100 000 vibration cycles. In the meanwhile, the electricity generation on the PTFE based REWOD-DEG presents obvious deterioration with the time, in particular at high bias voltages. The contrasting results improve the effective ion-blocking effect of the SLIPS, which supports the long-term running stability of the system.

To prove the self-healing potential coming from SLIPS, the DEG performances before and after physical scratching were studied. In its original state, the lubricant with ultra-low surface energy wets and fills the porosity, and further forms a defect-free complete film (Fig. 4b). Thanks to the fluidic nature of the SLIPS, once encountering physical damage, the wound can be self-healed by nearby lubricant through capillary wicking effect and high mobility. In our experiments, the light scratches on the surface repaired themselves within 1 second. After 20 minutes, the SLIPS was completely self-healed (Movie S1†). The power generation performance of the DEG before and after scratching (Fig. 4c) is comparable, which demonstrates the immunity of SLIPS covered DEG to physical damage.[23] To further investigate the stability of power generation of SLIPS, intermittent REWOD-DEG energy harvesting tests were performed over a period of 100 days, and no weakening of the output voltage was observed (Fig. 4d).

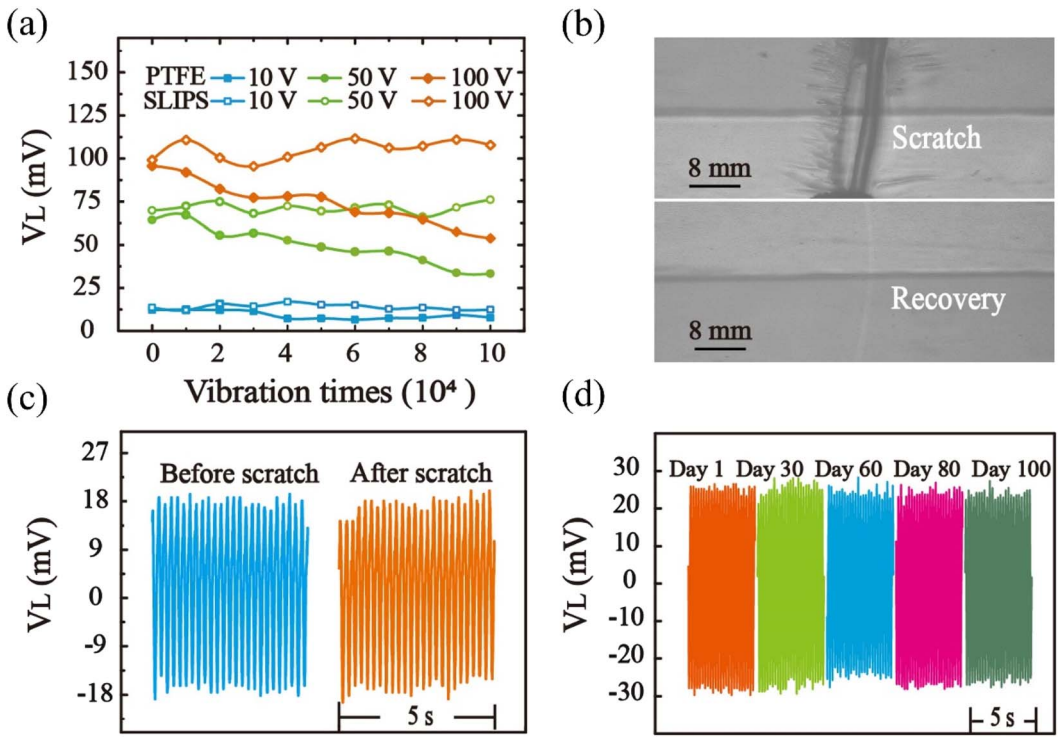

Fig. 4 The stability of power generation for SLIPS based REWO-DEG. (a) Long-term operating stability with one hundred thousand vibrations under different bias voltages. (b) The scratching damage of SLIPS can be restored within 20 minutes. (c) The output V_L of the SLIPS based REWOD-DEG shows no decline after scratching test. (d) Long-term running performance for 100 days. $R_L = 10$ MΩ, $L = 1.2$ mm, $f = 5$ Hz.

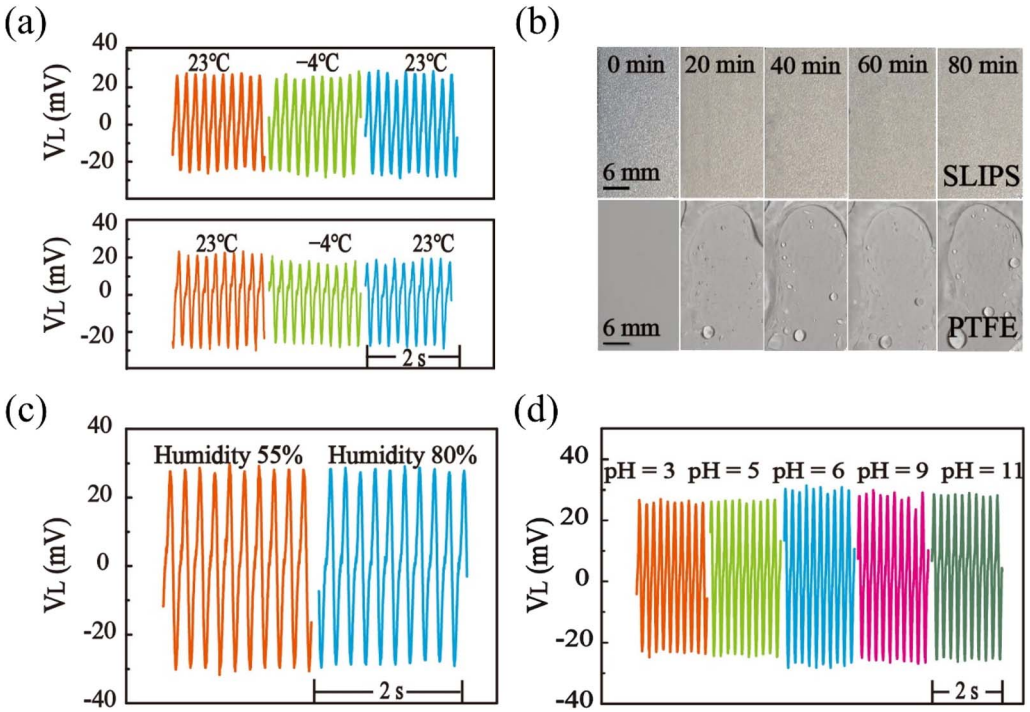

Fig. 5 Extreme condition test. (a) SLIPS based REWOD-DEG performed (upper set of data) more stable under low temperature compares to PTFE based device. (b) SLIPS shows antiicing merit at low temperatures, and the impinging droplet slides off in a timely manner. In contrast, a droplet impinging on PTFE was easily pinned because of the formation of ice layer. The release height was 30 cm and the flow rate was 5 mL min^{-1}. (c) Stable power generation under high humidity conditions. (d) pH tolerance test. For all graphs the droplet volume is 10 μL, bias voltage = 20 V, R_L = 10 MΩ, L = 1.2 mm, f = 5 Hz.

SLIPS in extreme environments such as low temperature, high humidity, and acid–base conditions, lubricant injection still allows for excellent stability.[40–42] At room temperature (23 °C), SLIPS produces a slightly higher V_L than PTFE (Fig. 5a), which is consistent with our conclusion above that SLIPS has a lower charge trapping rate. The two samples were then placed on a cooling platform at −4 °C and tilted 45°. Droplets were released directly over the samples with an injection pump, and ice coverage was recorded every 20 minutes with a camera. Remarkably, during the 80 minute test, the surface of SLIPS became less transparent only due to the condensation of water vapor in the air, and due to the ultra-smooth nature of the surface, no ice formed that would have resulted from the release of droplets. PTFE, on the other hand, exhibited many small condensation droplets and a layer of ice after 20 minutes, and the ice formation became more evident as the test duration progressed (Fig. 5b and Movie S2†). We immediately REWOD-DEG the two samples tested at low temperature and found that PTFE performance decreased significantly because the ice layer prevented effective charge transfer on the surface. After that, samples are thawed at room temperature for 1 hour before REWOD-DEG. SLIPS still maintain stable output and have good low temperature resistance. However, the adhesion between PTFE and ITO substrate is obviously weakened after this process, the energy harvesting effect is affected by the failure to maintain steady contact with the droplet during vibration.

Similarly, when considering practical applications such as energy harvesting during the rainy season, the lifetime of the superhydrophobic surface is susceptible to excessive humidity.[41–43] Therefore, we mimicked the conditions for energy harvesting at normal humidity (55%) and humidity during the rainy season (80%) at room temperature (23 °C) (Fig. 5c). The results demonstrate that SLIPS maintain stable output even in high humidity environments, without experiencing attenuation phenomena. Benefit from the excellent chemical inertness, liquid repellency and "slippery" properties, the SLIPS based REWOD-DEG can work with droplets over a wide range of pH (Fig. 5d). In addition, it also shows anti-fouling properties, which can realize self-cleaning (Fig. S5†) and repelling complex liquids (Fig. S6†). The above results clearly demonstrated that the introduction of SLIPS effectively improves the stability of REWOD-DEG.

3 Conclusion

In this paper, a lubricant-infused porous surface (SLIPS) is introduced in the reversed-electrowetting based droplet electricity generator (REWOD-DEG), which has low contact angle hysteresis and low charge trapping characteristics and is capable of stable power generation for a long time at high bias voltage. Based on vibrating plate type REWOD-DEG, adjusting the conductive droplet concentration, vibration frequency and vibration amplitude to regulate the output power, the best

matching load of the system was obtained, and the maximum output power of the generator was 143 nW. The SLIPS enhanced REWOD-DEG experienced 100 days of intermittent energy harvesting with no degradation in performance. In addition, when exposed to a variety of extreme operating conditions, such as low temperature, pH, humidity, fouling, and even scratching, the device shows robust performance.

4 Methods

4.1 Preparation of SLIPS

A clean indium tin oxide (ITO) electrode is prepared, anhydrous ethanol drops are added to the plate, and then a porous polytetrafluoroethylene (PTFE) film is covered. With the evaporation of anhydrous ethanol, PTFE adhered closely to the electrode by capillary force, which showed strong mechanical stability in the experiment. Krytox fluorinated oil was spin-coated on PTFE film at 1500 rpm, and the lubricant spontaneously infiltrated into the film to form a smooth oil film. With an average pore diameter of 200 nm, a thickness of 20 μm, and a solid phase ratio of 0.16. A perfluorinated liquid (DuPont Krytox GPL103, surface tension $\gamma = 16$–20 mN m^{-1}) was chosen as the lubricant.

4.2 Surface charging test

The SLIPS and PTFE samples were immersed in an aqueous solution at a uniform speed using a dip-lift coater. A voltage of 400 V was applied between the sample electrodes and the solution. At this time, no degradation has occurred in the sample, allowing charging by electrowetting assisted charge injection. After charging, the sample was subjected to an electrowetting curve test to determine the amount of trapped charge.

4.3 REWOD-DEG experimental apparatus and measurement methods

As shown in Fig. S7,† the experimental setup for REWOD-DEG based vibration energy harvesting was mainly composed of a standard shaking table (KSI-758ST50, KingSci, Inc.) with adjustable vibration amplitude and frequency, a power supply unit (waveform generator, DG-1032, Rigol, Inc. and signal amplifier ATA-2161, Agitek, Inc.) and signal measurement & display unit (Oscilloscope MSO7054B, Agilent, Inc. and phase-locked amplifier OE1022, Sine Scientific, Inc.). The voltage distributed on the load resistance V_L was timely acquisited. V_{rms} is the root mean square value of V_L. A high-speed camera was used to capture the vibration amplitude L through image and the calculation software. The gap between the conductive droplet and the upper plate was controlled by a lifting platform.

Author contributions

B. T. conceived the idea and supervised the project. H. C. conducted the experiments with supports from W. S. and J. W. B. T. and H. C. led the data analysis and manuscript writing integrated the contributions from J. J., M. Z. and G. Z. All authors reviewed the manuscript.

Conflicts of interest

There are no conflicts to declare.

Acknowledgements

We appreciate the financial support from National Key R&D Program of China (2021YFB3600602), National Natural Science Foundation of China (52175403), the National R&D Program of China (zcgx2022002L), Program for Guangdong Innovative and Enterpreneurial Teams (No. 2019BT02C241), Guangdong Provincial Key Laboratory of Optical Information Materials and Technology (2017B030301007), Guangzhou Key Laboratory of Electronic Paper Displays Materials and Devices (201705030007), MOE International Laboratory for Optical Information Technologies, and the 111 Project.

References

1 N. Zhang, H. Gu, H. Zheng, S. Ye, L. Kang, C. Huang, *et al.*, Boosting the output performance of volume effect electricity generator (VEEG) with water column, *Nano Energy*, 2020, **73**, 104748, DOI: **10.1016/j.nanoen.2020.104748**.

2 F. Invernizzi, S. Dulio, M. Patrini, G. Guizzetti and P. Mustarelli, Energy harvesting from human motion: materials and techniques, *Chem. Soc. Rev.*, 2016, **45**, 5455–5473, DOI: **10.1039/c5cs00812c**.

3 Z. Chen, J. Shi, Y. Li, B. Ma, X. Yan, M. Liu, *et al.*, Recent progress of energy harvesting and conversion coupled with atmospheric water gathering, *Energy Convers. Manage.*, 2021, **246**, 114668, DOI: **10.1016/j.enconman.2021.114668**.

4 A. Harb, Energy harvesting: state-of-the-art, *Renewable Energy*, 2011, **36**, 2641–2654, DOI: **10.1016/j.renene.2010.06.014**.

5 U. Khan and S.-W. Kim, Triboelectric nanogenerators for blue energy harvesting, *ACS Nano*, 2016, **10**, 6429–6432, DOI: **10.1039/c5cs00812c**.

6 W. Tang, T. Jiang, F. Fan, A. Yu, C. Zhang, X. Cao, *et al.*, Liquid-metal electrode for high-performance triboelectric nanogenerator at an instantaneous energy conversion efficiency of 70.6%, *Adv. Funct. Mater.*, 2015, **25**, 3718–3725, DOI: **10.1002/adfm.201501331**.

7 S. Pan and Z. Zhang, Fundamental theories and basic principles of triboelectric effect: a review, *Friction*, 2018, **7**, 2–17, DOI: **10.1007/s40544-018-0217-7**.

8 Y. Yang, Y. Zhou, H. Zhang, Y. Liu, L. Sangmin and Z. Wang, A single-electrode based triboelectric nanogenerator as self-powered tracking system, *Adv. Mater.*, 2013, **25**, 6594–6601, DOI: **10.1002/adma.201302453**.

9 J. Yang and D. Y. Kwok, Microfluid flow in circular microchannel with electrokinetic effect and Navier's slip condition, *Langmuir*, 2003, **19**, 1047–1053, DOI: **10.1021/la026201t**.

10 T. G. Yun, J. Bae, A. Rothschild and I.-D. Kim, Transpiration driven electrokinetic power generator, *ACS Nano*, 2019, **13**, 12703–12709, DOI: **10.1021/acsnano.9b04375**.

11 D. Hu, M. Yao, Y. Fan, C. Ma, M. Fan and M. Liu, Strategies to achieve high performance piezoelectric nanogenerators, *Nano Energy*, 2019, **55**, 288–304, DOI: **10.1016/j.nanoen.2018.10.053**.

12 R. Yang, Y. Qin, L. Dai and Z. Wang, Power generation with laterally packaged piezoelectric fine wires, *Nat. Nanotechnol.*, 2008, **4**, 34–39, DOI: **10.1038/nnano.2008.314**.

13 J. K. Moon, J. Jeong, D. Lee and H. K. Pak, Electrical power generation by mechanically modulating electrical double layers, *Nat. Commun.*, 2013, **4**, 1487, DOI: **10.1038/ncomms2485**.

14 P. Simon and Y. Gogotsi, Materials for electrochemical capacitors, *Nat. Mater.*, 2008, **7**, 845–854, DOI: **10.1038/nmat2297**.

15 J. Yu, E. Ma and T. Ma, Harvesting energy from low-frequency excitations through alternate contacts between water and two dielectric materials, *Sci. Rep.*, 2017, **7**, 17145, DOI: **10.1038/s41598-017-17522-8**.

16 T. Krupenkin and J. A. Taylor, Reverse electrowetting as a new approach to high-power energy harvesting, *Nat. Commun.*, 2011, **2**, 448, DOI: **10.1038/ncomms1454**.

17 T.-H. Hsu, S. Manakasettharn, J. A. Taylor and T. Krupenkin, Bubbler: a novel ultra-high power density energy harvesting method based on reverse electrowetting, *Sci. Rep.*, 2015, **5**, 16537, DOI: **10.1038/srep16537**.

18 H. Yang, S. Hong, B. Koo, D. Lee and Y.-B. Kim, High-performance reverse electrowetting energy harvesting using atomic-layer-deposited dielectric film, *Nano Energy*, 2017, **31**, 450–455, DOI: **10.1016/j.nanoen.2016.11.006**.

19 G. Kim, W. Kim and H. Chun, Droplet energy harvesting is reverse phenomenon of electrowetting on dielectric, *Adv. Funct. Mater.*, 2021, **31**, 2105233, DOI: **10.1002/adfm.202105233**.

20 P. R. Adhikari, N. T. Tasneem, R. C. Reid and I. Mahbub, Electrode and electrolyte configurations for low frequency motion energy harvesting based on reverse electrowetting, *Sci. Rep.*, 2021, **11**, 5030, DOI: **10.1038/s41598-021-84414-3**.

21 C. Hao, Y. Liu, X. Chen, Y. He, Q. Li, K. Y. Li, *et al.*, Electrowetting on liquid-infused film (EWOLF): complete reversibility and controlled droplet oscillation suppression for fast optical imaging, *Sci. Rep.*, 2014, **4**, 6846, DOI: **10.1038/srep06846**.

22 J. Jiang, J. Gao, H. Zhang, W. He, J. Zhang, D. Daniel, *et al.*, Directional pumping of water and oil microdroplets on slippery surface, *Proc. Natl. Acad. Sci. U.S.A.*, 2019, **116**, 2482–2487, DOI: **10.1073/pnas.1817172116**.

23 W. Xu, X. Zhou, C. Hao, H. Zheng, Y. Liu, X. Yan, *et al.*, SLIPS-TENG: robust triboelectric nanogenerator with optical and charge transparency using a slippery interface, *Natl. Sci. Rev.*, 2019, **6**, 540–550, DOI: **10.1093/nsr/nwz025**.

24 T. Guo, P. Che, L. Heng, L. Fan and L. Jiang, Anisotropic slippery surfaces: electric-driven smart control of a drop's slide, *Adv. Mater.*, 2016, **28**, 6999–7007, DOI: **10.1002/adma.201601239**.

25 X. Yuan, B. Tang, J. Barman, J. Groenewold and G. Zhou, Approximately symmetric electrowetting on an oil-lubricated surface, *RSC Adv.*, 2020, **10**, 20257–20263, DOI: **10.1039/D0RA02405h**.

26 J. Li, E. Ueda, D. Paulssen and P. A. Levkin, Slippery lubricant-infused surfaces: properties and emerging applications, *Adv. Funct. Mater.*, 2019, **29**, 1802317, DOI: **10.1002/adfm.201802317**.

27 M. H. Kim, H. Kim, K. S. Lee and D. R. Kim, Frosting characteristics on hydrophobic and superhydrophobic surfaces: A review, *Energy Convers. Manage.*, 2017, **138**, 1–11, DOI: **10.1016/j.enconman.2017.01.067**.

28 H. Wu, N. Mendel, S. van der Ham, L. Shui, G. Zhou and F. Mugele, Charge trapping-based electricity generator (CTEG): an ultra robust and high efficiency nanogenerator for energy harvesting from water droplets, *Adv. Mater.*, 2020, **32**, 2001699, DOI: **10.1002/adma.202001699**.

29 H. Wu, N. Mendel, D. van den Ende, G. Zhou and F. Mugele, Energy harvesting from drops impacting onto charged surfaces, *Phys. Rev. Lett.*, 2020, **125**, 078301, DOI: **10.1103/physrevlett.125.078301**.

30 H. J. J. Verheijen and M. W. J. Prins, Reversible electrowetting and trapping of charge: model and experiments, *Langmuir*, 1999, **15**, 6616–6620, DOI: **10.1021/la990548n**.

31 L. Gao and T. J. McCarthy, Contact angle hysteresis explained, *Langmuir*, 2006, 6234–6237, DOI: **10.1021/la060254j**.

32 S. Qiao, S. Li, Q. Li, B. Li, K. Liu and X.-Q. Feng, Friction of droplets sliding on microstructured superhydrophobic surfaces, *Langmuir*, 2017, **33**, 13480–13489, DOI: **10.1021/acs.langmuir.7b03087**.

33 T. Gilet, D. Terwagne, N. Vandewalle and S. Dorbolo, Dynamics of a bouncing droplet onto a vertically vibrated interface, *Phys. Rev. Lett.*, 2008, **100**, 1678023, DOI: **10.1103/physrevlett.100.167802**.

34 M. Delmas, M. Monthioux and T. Ondarçuhu, Contact angle hysteresis at the nanometer scale, *Phys. Rev. Lett.*, 2011, **106**, 136102, DOI: **10.1103/PhysRevLett.106.136102**.

35 M. D. Dickey, Stretchable and soft electronics using liquid metals, *Adv. Mater.*, 2017, **29**, 1606425, DOI: **10.1002/adma.201606425**.

36 M. D. Dickey, Emerging applications of liquid metals featuring surface oxides, *ACS Appl. Mater. Interfaces*, 2014, **6**, 18369–18379, DOI: **10.1021/am5043017**.

37 G. Li, M. Parmar, D. Kim, J.-B. Lee and D.-W. Lee, PDMS based coplanar microfluidic channels for the surface reduction of oxidized Galinstan, *Lab Chip*, 2014, **14**, 200–209, DOI: **10.1039/c3lc50952d**.

38 J. M. Oh, S. H. Ko and K. H. Kang, Shape oscillation of a drop in ac electrowetting, *Langmuir*, 2008, **24**, 8379–8386, DOI: **10.1021/la8007359**.

39 D. K. Davies, Charge generation on dielectric surfaces, *J. Appl. Phys.*, 1969, **2**, 1533–1537, DOI: **10.1088/0022-3727/2/11/307**.

40 K. K. Varanasi, T. Deng, J. D. Smith, M. Hsu and N. Bhate, Frost formation and ice adhesion on superhydrophobic surfaces, *Appl. Phys. Lett.*, 2010, **97**, 234102, DOI: **10.1063/1.3524513**.

41 S. Amini, S. Kolle, L. Petrone, O. Ahanotu, S. Sunny, C. N. Sutanto, *et al.*, Preventing mussel adhesion using lubricant-infused materials, *Science*, 2017, **357**, 668–673, DOI: **10.1126/science.aai8977**.

42 X. Tian, T. Verho and R. H. A. Ras, Moving superhydrophobic surfaces toward real-world applications, *Science*, 2016, **352**, 142–143, DOI: **10.1126/science.aaf2073**.

43 R. Feng, C. Xu, F. Song, F. Wang, X. Wang and Y. Wang, A Bioinspired slippery surface with stable lubricant impregnation for efficient water harvesting, *ACS Appl. Mater. Interfaces*, 2020, **12**, 12373–12381, DOI: **10.1021/acsami.0c00234**.